Journal of Imaging Science and Technology® 57(6): 060503-1–060503-8, 2013.

Aggregation Behavior of Colloidal Particles for Production of Polyester-Based Chemically Prepared Toner

Sung Yul Kim
Advanced Material R&D Center, Samsung Fine Chemicals Co., Ltd., 103-1, Moonji-Dong, Yusung-Gu, Daejeon, 305-380, Korea
E-mail: sungyul.kim@samsung.com

Bo Young Kim
Corporate Planning Team, Samsung Fine Chemicals Co., Ltd., 1320-10 Seocho 2-Dong, Seocho-Gu, Seoul, 135-857, Korea

Kyung-Yol Yon
Advanced Material R&D Center, Samsung Fine Chemicals Co., Ltd., 103-1, Moonji-Dong, Yusung-Gu, Daejeon, 305-380, Korea

Abstract. *High performance, full color electrophotographic printers are gaining acceptance in many office environments. In this study, the authors controlled the aggregation of three different colloidal dispersions using four different multivalent metallic coagulants over a wide pH range to develop a polyester-based chemically prepared toner (CPT). An operational limit existed for the total quantity of each metallic coagulant required to achieve a narrow particle size distribution at a mean target aggregate size. This, when exceeded, produced a viscous, inoperative sludge in the reactor. The optimal pH condition for each coagulant system was mainly dependent on the electrostatic balance produced by deprotonation of exposed carboxylic acid groups on the polyester resin particles at a pH between 5.5 and 6.5. Additional electrostatic interactions between the polyester colloidal dispersions and the monovalent cations ($M1^{+}$) in the metallic coagulation system at high electrolyte concentrations created a favorable environment to reproduce core-toner particles with a narrow particle distribution at a mean target size. By manipulating the aggregation process, the individual nano-dispersions coalesced in an aqueous environment to form a polyester-resin-based chemical toner that was uniform in particle size and had low total volatile organic compound (VOC) level. The printing and image performance of this toner using a color laser printing system was also observed. This final polyester toner was optimized for high speed, energy efficient electrophotographic printers that utilize an oil-free fusing subsystem that operates at a low fusing temperature. The image quality and toner usage of these toners meet the specifications of major printer manufacturers for digital printing technologies.* © *2013 Society for Imaging Science and Technology.*
[DOI: 10.2352/J.ImagingSci.Technol.2013.57.6.060534]

INTRODUCTION

Over the past few years, major manufacturers of office color and monochrome laser printers are moving away from traditional melt-pulverized toner (MPT) to chemically manufactured or polymerized toner. Compared to conventional MPT, chemically prepared toner (CPT) provides more precise control over the morphology (size distribution, shape, surface structure) of individual toner particles.[1,2]

The use of polyester binder resin in toner for high speed digital printing applications is highly desirable because of its melt rheology and mechanical toughness at low melt viscosities. Internal hydrogen bonding between hydroxyl groups and carboxylic acids within the polyester resin provides the toner with enhanced mechanical strength, viscoelasticity, and thermal properties.[3] The alternative vinyl polymer binders are quite brittle at the low molecular weights which are necessary to achieve a high gloss and color saturation. As a consequence, most styrene-acrylate-based toners have higher melt viscosities and provide lower gloss prints than polyester-based toners.[4]

However, the manufacturing methods of polyester-based CPT are not well understood and many of the commercially available methods involve solvent-based processes, including Suspension of Polymer/pigment Solution Solvent removal (SPSS, Fuji Xerox), Polyester Polymerization (PxP, Sanyo and Ricoh), and Chemical Milling (CM, DPI Solutions).[4,5] The emulsion aggregation (EA) process is the most widely used preparation method for styrene-acrylate-based CPT production. This method is regarded as being highly reproducible and environmentally friendly because the overall process is conducted in the aqueous phase. However, in spite of the benefits, the aggregation of colloidal particles in an aqueous phase like the EA process has not been applied much to polyester-based CPTs except EA-Eco toner (Fuji Xerox),[6] and the aggregation behavior of polyester colloidal particles is not well understood.

An understanding of the interaction forces between colloidal particles and their aggregation processes is crucial, not only for industrial applications, but also for biomedical applications.[7] These forces depend on the various process parameters needed to control and optimize the aggregation of dissimilar polyester, wax, and pigment dispersions. Through the manipulation of the various preparation parameters, including ionic strength, pH, temperature, viscosity, shear force, and zeta potential, the growth and aggregation of polyester-based colloidal particles in the aqueous phase was controlled to achieve toner particles of a desired target size. The Derjaguin–Landau–Verwey–Overbeek (DLVO) theory was used to describe and explain the ionic interactions be-

---

Received Jan. 11, 2013; accepted for publication Dec. 9, 2013; published online Jan. 13, 2014. Associate Editor: Hiroyuki Kawamoto.
1062-3701/2014/57(6)/060503/8/$25.00

tween the different colloids and various metallic coagulants used.

In this article, we present a polyester colloid aggregation process which is able to manufacture better performance polyester-based chemical toners with both uniform and narrow size distribution.[8] The toner offers both improved print quality and environmental stability as well as combined benefits of polyester resins and chemical toners.

EXPERIMENTS

Synthesis of Polyester Resin

Polyester resin for the CPT was prepared as described in Kim, et al.[9] Briefly, a reactor equipped with a stirrer, nitrogen gas inlet, thermometer, and cooler was installed in an oil bath heat transfer medium. The reactor was charged with 28% (w/w) terephthalic acid, 24% (w/w) isophthalic acid, 46% (w/w) 1,2-propylene glycol, and 2% (w/w) trimellitic acid (all chemicals purchased from Duksan Pure Chemical Co., Korea), and tetrabutyl titanate (Sigma-Aldrich, USA) was added as a catalyst at a ratio of 500 ppm with respect to the total weight of the monomers. The reactor was maintained at 150°C for 6 h with impeller stirring at 150 rpm. Subsequently, the reactor temperature was increased to 220°C and the pressure reduced to 0.1 Torr in order to remove reaction byproducts. The reactor was maintained in this state for 15 h to yield solid polyester resin.

Preparation of Polyester Resin Dispersion

A mixture of 0.6% (w/w) sodium hydroxide (Samsung Fine Chemical Co. Ltd., Korea) as the dispersion stabilizer, 1% (w/w) Dowfax 2A1 surfactant (Dow Corning Co. Ltd., USA), and 2.5 equivalents of deionized water with respect to the amount of polyester resin was added to a reactor equipped with a thermometer and an impeller-type stirrer. After that, 98.4% (w/w) solid polyester resin was added to the reactor and 2.5 equivalents of methyl ethyl ketone (Samchun Pure Chemical Co., Korea) relative to the amount of polyester resin was slowly added to the reactor. The mixture was refluxed at 70°C for 1 h and the organic solvent was removed while purging with nitrogen at 90°C for a period of more than 4 h.

Preparation of Pigment Dispersion

A mixture of 95% (w/w) cyan pigment (ECB303, Daicolor Pigment MFG. Co., Ltd., Japan), 5% (w/w) surfactant, and 4.0 equivalents of deionized water with respect to pigment was added to a reactor equipped with a stirrer, thermometer, and condenser. The reactor was slowly stirred for about 10 h to prepare the pre-dispersion. The pre-dispersion was then dispersed four times at 1,500 bar using an Ultimaizer (Armstec Ind. Co. Ltd., Korea) until particle size measured no more than 200 nm using a Microtrac 252 (Microtrac Inc., USA), forming a cyan pigment dispersion. The same procedure was applied to the other colors: magenta, yellow, and black.

Preparation of Wax Dispersion

A mixture of 95% (w/w) C-80 paraffin wax (Sasol, South Africa, melting point: 84°C), 5% (w/w) an anionic surfactant (sodium dodecylbenzenesulfonate, Rhodia, France), and 2.7 equivalents of deionized water with respect to the wax was added to a jacket reactor and the mixture was dispersed at 95°C for 30 min using a homogenizer (IKA Works, USA). The emulsion mixture was added to a pressure-ejecting homogenizer (Japan Precision Instruments Inc., Japan) and dispersed at 90°C for about 20 min to obtain a wax dispersion having a volume average particle size of 230 nm (D50(v)) obtained using a Microtrac 252 sizing instrument (Microtrac Inc., USA).

Preparation of Toner Particles

A reactor was charged with 90% (w/w) of the polyester resin dispersion, 5% (w/w) of the pigment dispersion, and 5% (w/w) of the wax dispersion. These amounts are based on solid content and the total solid content was adjusted to 13% (w/w) using deionized water. Various amounts of metallic coagulants, $M1^{+1}$, $M2^{+2}$, $M3^{+2}$, and $M4^{+3}$ (coagulant type is confidential), and a 0.3 M nitric acid solution were added to the mixture. The mixture was heated to 52°C and stirred using a blend-type stirrer at 10,000 rpm for about 3 h to grow the aggregates from the individual colloids. This unstable aggregate mixture was treated with 1 N sodium hydroxide solution to prevent additional aggregation (freezing) and heated to 95°C to agglomerate (coalesce) the core-toner particles. When the circularity of the core-toner particles was greater than 0.985, the mixture was cooled to 60°C and the pH of the mixture was adjusted to 9 by adding a 1 N sodium hydroxide solution. After the mixture reached room temperature, the coarse particles were removed using a 20 μm mesh size filter and the harvested particles were washed with deionized water. A 0.3 M nitric acid solution was added to adjust the pH to 1.5 and the resultant was washed and filtered again. The filtrate was dried using a fluidized bed dryer to prepare the core-toner particles.

Analysis of Average Diameter, Geometric Size Distribution, and Circularity of Particles

The reactants and dispersed toner particles were diluted in an isotonic solution and analyzed using a Multisizer IV® (Beckman Coulter, Inc. USA) with a 100 μm aperture to perform statistical analysis on 50,000 core-toner particles. Circularity was measured by dispersing the core-toner particles in ionized water and analyzed using an FPIA-3000 sizing instrument (Sysmex, Japan). The geometric size distributions (GSDp, GSDv) and circularity are tabulated in Table I.

Analysis of SEM, TEM, and 3D Electron Tomography

Scanning electron microscopy (SEM) images were acquired using a JSM-7400 F (JEOL, Japan) in the LEI detector mode. A series of transmission electron microscopy (TEM) images were reconstructed to form 3-dimensional electron

Table I. Particle formation parameters of the Samsung Fine Chemicals (SFC)-CPT.

	Target	OEM-CPT	MPT
D50(v)[a]	**6.20 ± 0.30**	6.18 ± 0.27	6.04 ± 1.10
GSDp[b]	≤**1.300**	1.25 ± 0.01	1.41 ± 0.11
GSDv[c]	≤**1.300**	1.21± 0.01	1.32 ± 0.10
Circularity[d]	≥**0.985**	0.985 ± 0.002	0.943 ± 0.025

[a] Average particle diameter (μm).

[b] Geometric size distribution of number (n) data where $GSD_p = (D84, n/D16, n)^{1/2}$.

[c] Geometric size distribution of volume (v) data where $GSD_v = (D84, v/D16, v)^{1/2}$.

[d] Ratio of circle circumference to perimeter of projected particle image; circularity $= 2 \times (\text{area} \times \pi)^{1/2}/\text{perimeter}$.

tomography images.[10] Thin film cross-sections of the core-toner particles, which were coated and embedded in a solid continuous phase, were prepared using a ultramicrotome (Powertome MT, RMC). The internal components were observed using TEM operating at 200 kV with a field-emission gun (Tecnai F20st, FEI) and at 1.25 MeV with a tungsten filament (JEM-ARM 1300S, JEOL, Japan).

Analysis of Total Volatile Organic Compounds (TVOC)

The amount of TVOC was analyzed and certified by Landesgewerbeanstalt Bayern (LGA, third party test institute whose tests meet the requirements of the Blue Angel Award standard) based on the "LGA-tested for contaminants." The sample was analyzed by thermoextraction and subsequent thermodesorption GC/MS.[11]

Evaluation of Image Quality and Printing Performance

Dried core-toner was surface-treated with a mixture of both large and small external silica additives (additive type and composition are confidential). An IAS® image quality analysis system (QEA, USA) and SpectroEye® densitometer (X-rite, USA) were used to evaluate electrophotographic print quality using in-house procedures based on the International Organization for Standardization (ISO) and the American Society for Testing and Materials (ASTM).

Statistical Analysis

The Minitab13 statistical analysis software package (Minitab Inc. USA) was used to perform a Pearson correlation analysis to measure the degree of linearity (presented as Pearson correlation coefficient: r) between two variables. An r-value higher than 0.3 signifies a clear quantitative correlation.

RESULTS AND DISCUSSION

Experimental & Particle Formation Parameters

The polyester resin, pigment, and wax dispersions were mixed together to produce toner particles through a process which controls size and shape. The control of the process parameters allows the individual sub-micron particles to form a core-toner particle with a targeted diameter, size distribution, shape, and surface structure.

Table I tabulates the particle morphology for three different types of toner particles as well as SFC's in-house target specifications. SFC toner offers a narrow particle size distribution and a uniform shape which is comparable to a leading OEM toner sample.

Aggregation of Polyester Colloidal Particles using Various Metallic Coagulants: Particle Size Distribution

Polyester colloidal particles are lyophobic colloids that are distinguished from lyophilic colloids in part by the sensitivity of the dispersion to electrolytes and the use of surfactants or dispersants to stabilize the dispersion. The stability of polyester colloidal particles in solution is controlled by a combination of electrostatic repulsion and London–van der Waals attraction forces, as described by the DLVO theory of colloidal stability.[7,12] Figure 1 shows the aggregation of polyester, wax, and pigment dispersions as a result of the addition of metallic coagulants. In Fig. 1, the characteristics and amounts of metallic coagulants are depicted by arbitrary coagulant numbers and concentration units with the exception of the valence of the metal ions. For example, $M3^{+2}$ represents metallic coagulant #3 with a divalent ion.

As shown in Figs. 1A and B, quite different quantities of coagulants were required to form the aggregated particles. A different working concentration for each metal coagulant was required to achieve the narrow particle size distribution. The unique quantity of each metal coagulant was highly dependent on the valence number of the metallic coagulant ion. This observation is in agreement with the empirically derived Schulze–Hardy rule[13] stating that hydrophobic colloids flocculate most efficiently by ions with high charge number. Introduction of small quantities of metal coagulants with a higher valence number ($M4^{+3}$) significantly increased the viscosity of the reactant when compared to metal coagulants with a lower ion valence number ($M1^{+}$) due to severe colloid aggregation

In addition, *an operational limit existed for the total quantity of each metallic coagulant required to achieve a narrow particle size distribution at a mean target aggregate size. This, when exceeded, produced a viscous, inoperative sludge in the reactor*, as shown in Figs. 1A and B. The quantitative dependences of $M1^{+}$ (only GSDp), $M2^{+2}$, and $M4^{+3}$ on particle size distribution were statistically significant.

Figs. 1C and D show that the particles aggregated over a broad pH range and varied with the type of metallic coagulant. Moreover, the dependence of the aggregated particle distributions on pH overlapped and converged at pH 5.5–6.5 for all of the coagulants. In general, the cationic charge of high valent metallic coagulants decreases with increasing pH so that their coagulation power can be controlled by pH. For example, ferric ions (Fe^{3+}) form hydroxyl ferric complex ions as the pH increases, that is, $Fe(OH)^{2+} + 3(OH)^{-1} \leftrightarrows Fe(OH)_2^{+1} + 2(OH)^{-1} \leftrightarrows Fe(OH)_3 + (OH)^{-1} \leftrightarrows Fe(OH)_4^{-1}$.[14] Aluminum ions ($Al^{3+}$) also form hydroxyl aluminum complex ions as the pH increases: $Al_8(OH)_{20}^{4+}$, Al^{3+}, $Al(OH)^{2+}$, $Al(OH)_2^{+}$, $Al(OH)_3$, and $Al(OH)_4^{-}$.[15] Even though it is generally more favorable for particles to aggregate when using multivalent metallic

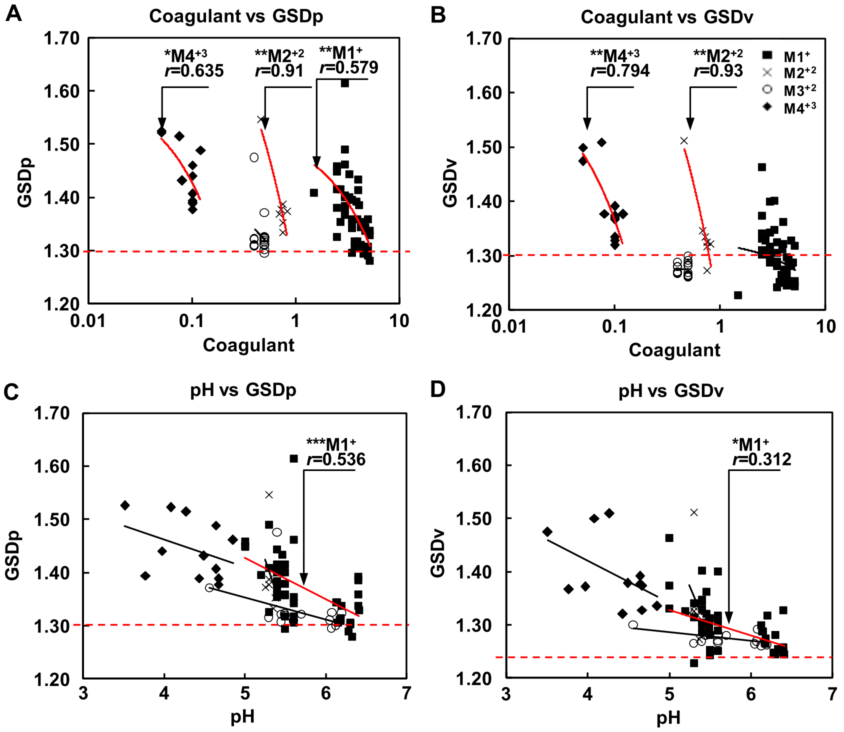

Figure 1. Aggregation behavior of polyester colloidal particles by the various metallic coagulants. A and B represent the dose dependences of each metallic coagulant on the GSDp and GSDv of the aggregated particle distributions. C and D represent the pH dependences of each coagulating condition on the GSDp and GSDv of the aggregated particle distribution. A Pearson correlation coefficient with clear correlation ($r > 0.3$) was presented for each coagulant's data. $*P < 0.05$, $**P < 0.01$, and $***P < 0.001$ represent the results of reliabilities on correlation analysis.

coagulants under acidic conditions (pH less than 5.0 in Figs. 1C and D), aggregation is more controllable at a pH of about 6.0. Therefore, it was the pH condition, rather than the coagulation strength of the metallic coagulant, which was more critical in producing a narrow volumetric size distribution of aggregated polyester colloidal particles. Based on a solution chart for Fe^{+3} and Al^{+3} ions,[14,15] only the monovalent form of these metallic hydroxide ions (such as $Fe(OH)_2^+$ and $Al(OH)_2^+$) is largely available at a pH of about 6.0. This ionic form does not seem suitable to produce aggregated colloidal particles with a narrow size distribution. Similar behavior for divalent metallic ions is also reported.[16]

Amongst all the properties of polyester colloidal dispersions, the level of acidity is the most critical factor as it relates the pH dependence of aggregate particle formation. We observed that as the pH of the dispersion solution increased, the carboxylic acids exposed on the surface of polyester dispersions were ionized to carboxylates, and the stability and viscosity of the polyester dispersions increased. Due to the increased electrostatic interaction between the carboxylated functional groups on the polyester colloid surface and the metallic coagulant ions, colloidal aggregation seemed to be favorable in making aggregates with a narrow particle distribution.

Aggregation of Polyester Colloidal Particles using Various Metallic Coagulants: Particle Size Targeting

Figure 2 illustrates the particle size dependence based on the concentration of each coagulant and the pH of the solution. Fig. 2A shows that as the concentration of the $M1^+$ coagulant increased at a pH ~ 6.0, the toner particles converged to form small particle sizes. However, the colloid particle size could not be manipulated during the aggregation process to achieve the target size range using $M2^{+2}$ and $M4^{+3}$ coagulants (Figs. 2B and D). During this aggregation stage, neither the coagulant concentration nor the pH had any effect on reducing the particle size down to an acceptable level. Low solution viscosities at nearly neutral pH also indicated that aggregation had failed to occur (aggregation failure data were excluded from Figs. 2B and D). As discussed earlier, the valence number of metallic coagulants decreases around a neutral pH so that particles with both mean sizes below 6.5 μm and a narrow size distribution were not obtainable. With respect to $M3^{+2}$ (Fig. 2C), a metallic hydroxyl ion does not form at a pH of less than 7 (i.e., in acidic or neutral conditions), so small particle sizes with a narrow size distribution were attainable by the selection of the proper coagulant concentration under near pH neutral conditions (the in-house titration properties of $M3^{+2}$ coagulant agreed well with published results).[16] Table II summarizes the various coagulation systems and the conditions used to produce the polyester-based CPTs. A comparison of the D50, GSDp, and GSDv values shows that $M1^+$ was the best suited coagulant at this stage of the investigation. The $M3^{+2}$ coagulant was another good candidate for colloidal polyester aggregation but this system needs to resolve the issue with the elevated quantity of large aggregated particles (% particles

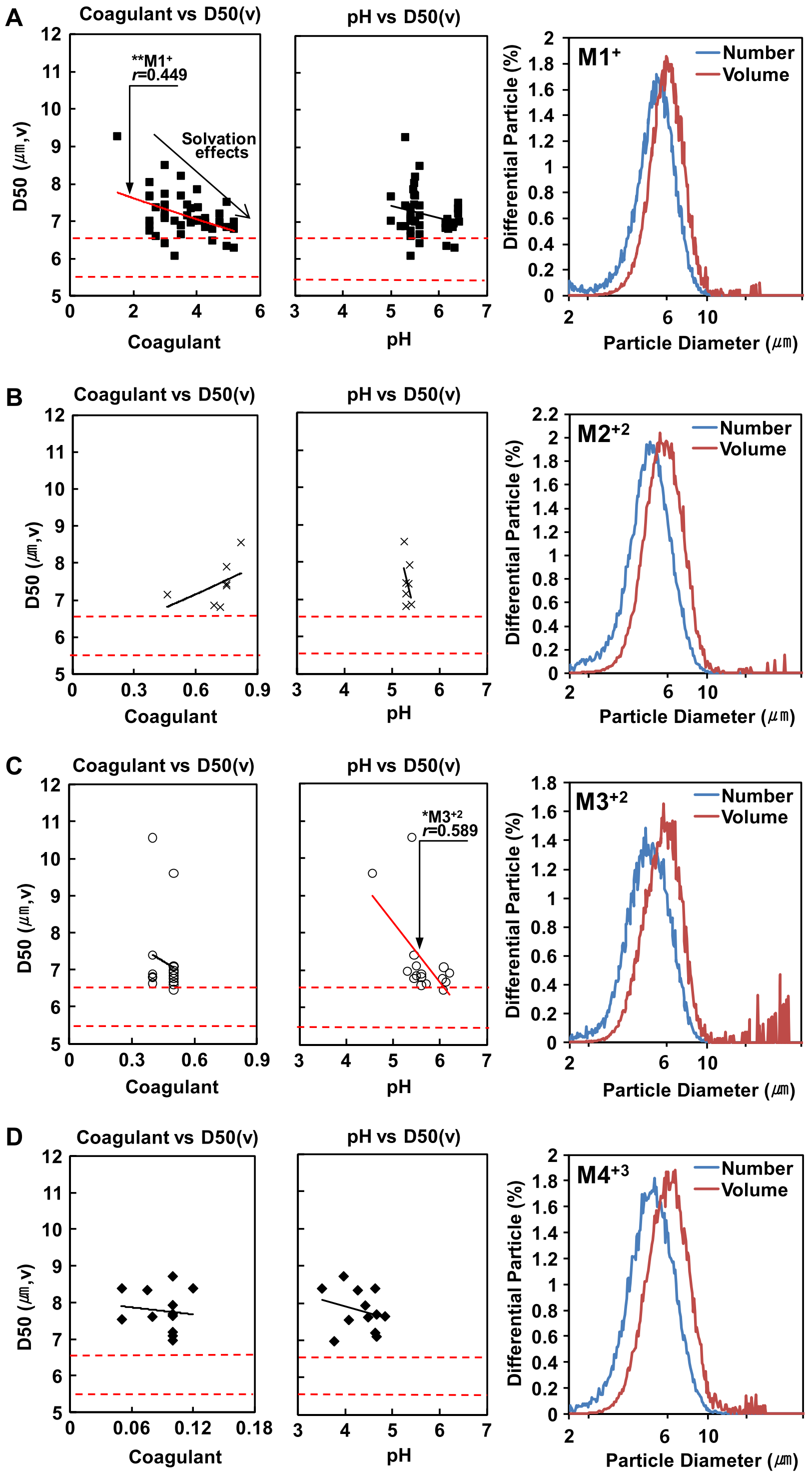

Figure 2. Manipulation of particle size for each aggregation system by the various metallic coagulants. The left and middle charts represent the dosage dependence of each metallic coagulant and pH dependence of each coagulating condition on the particle size of the colloidal aggregates. The right chart is a representative particle distribution for each coagulation system. A, B, C, and D represent the charts of $M1^{+}$, $M2^{+2}$, $M3^{+2}$, and $M4^{+3}$ coagulant, respectively. A Pearson correlation coefficient with clear correlation ($r > 0.3$) was presented for each coagulant's data. $*P < 0.05$ and $**P < 0.01$ represent the results of reliabilities on correlation analysis.

> 16 μm (v), Table II) before this option becomes viable. When the $M2^{+2}$ and $M4^{+3}$ aggregated samples were treated with a sodium hydroxide solution to prevent additional aggregation (freezing), the larger particles decreased in size: 7.4 μm → 5.9 μm, 7.2 μm → 6.2 μm respectively, due to the mechanical shearing force of the agitation process. In addition, the freezing step for divalent metallic coagulants required a chelator to prevent particle adhesion during the coalescing step. The residual chelator–metal salt complex may result in some electrostatic-related quality problems.

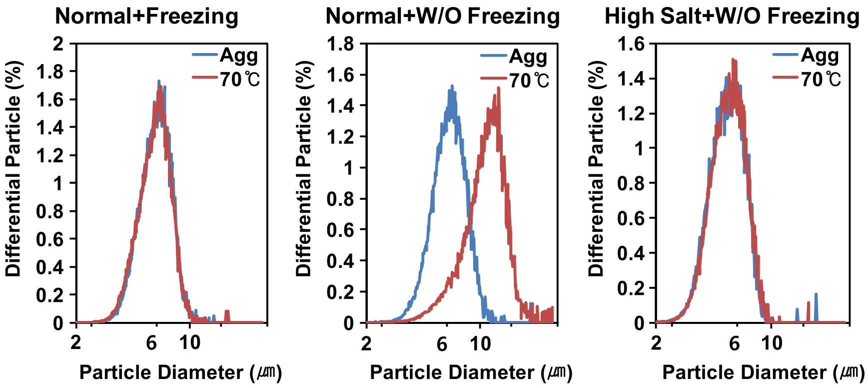

Figure 3. Effect of excessive M1$^+$ coagulant on the aggregation behavior of polyester colloidal particles. Each chart represents the particle distribution at the aggregation stage (Agg) and the pre-coalescence stage (70°C) either with or without (W/O) a freezing step. Normal is the representative condition of M1$^+$ coagulant and High Salt is the modified condition with increase of M1$^+$ coagulant by 20%.

Table II. Relative comparisons of polyester particle formations for each coagulation system.

Coagulant	M^{1+}	M2^{+2}	M3^{+2}	M4^{+3}
D50 (μm, v)	6.09	5.94	5.98	6.25
GSDp	1.25	1.27	1.28	1.30
GSDv	1.21	1.25	1.26	1.27
% of <3 μm (n)	3.28	3.96	3.28	3.19
% of >16 μm (v)	0.35	0.41	3.51	0.67
Freezing	pH	Chelation	Chelation	pH
Reproducibility & feasibility[a]	○	×[b]	△[c]	×[b]

[a] Reproducibility & feasibility were evaluated by the reproducibility of aggregation (Fig. 2) and the compatibility of the manufacturing process after the aggregation steps—that is, after freezing, coalescence, washing, and drying.

[b] Severe degradation of large particles was observed during the freezing and coalescence step.

[c] Moderate shrinkage and additional adhesion of particles was observed during freezing and coalescence step.

Effect of Solvation or Hydration Forces on the M1$^+$ *Coagulation System*

The aggregation behavior of the M1$^+$ coagulant system produced a more stable and reproducible aggregated particle than any other coagulation system investigated (as shown in Fig. 1, Fig. 2A, and Table II). In addition to coagulant mediated particle aggregation, repulsive forces between the M1$^+$ coagulant and aggregated particles were observed. When an excess amount of M1$^+$ coagulant was added to the system, particle growth was suppressed in spite of a change in the pH value. This phenomenon is depicted in Fig. 2A (marked with an additional arrowed line) and is referred to as the solvation effect or hydration force.[7] This is the interactive force that occurs between two charged surfaces when they approach each other at closer than a few nanometers. At such a close distance, their interactions in an aqueous solution fail to be explained by the DLVO theory.[17]

Figure 3 presents additional test results regarding the aggregation behavior of the M1$^+$ coagulant. Under an optimized M1$^+$ coagulant condition, we observed small particle sizes and a narrow toner particle distribution during the Normal + Freezing stage of the preparation process. Without the sodium hydroxide treatment, additional aggregation of the toner particles could occur when the process temperature was increased (Normal + W/O_Freezing). During agitation, colloidal particles may penetrate through the interfacial electrical double layer and coalesce only if the collision has sufficient energy to disrupt the charged surface layers. This disruption is more likely to occur at higher temperatures and is one reason why toner particles begin to aggregate at elevated temperatures without the freezing process.[18] However, the growth of toner particles without freezing (i.e., without sodium hydroxide treatment) was suppressed with an excess amount of M1$^+$ coagulant (High Salt + W/O Freezing). Under these conditions, the excess M1$^+$ ions produced a repulsive force at the surface that prevented any additional aggregation of the particles.

The aggregation conditions for the M1$^+$ coagulant were optimized for particle size and particle size distribution through a set of design of experiments (DOE), which are being used to develop our manufacturing processes for polyester-based chemically prepared toner (DOE data not shown).

Morphological Change of Particles After the Aggregation Step and Characteristics of SFC-Toner Particles

In addition to the narrow particle distribution, the SFC polyester-based CPT (SFC-CPT) has additional beneficial characteristics, including a uniform particle shape, uniform composite dispersion, controlled surface morphology, and core–shell structure. Figure 4 depicts the morphological changes that occur with SFC toners after the aggregation step in the manufacturing process. Aggregates of polyester colloidal particles (aggregation) begin to fuse with adjacent particles (early coalescence), fill the crevices between aggregates (intermediate coalescence), and coalesce into spherical shapes with a circularity value greater than 0.985 (final coalescence). The surfaces of the particles are very smooth and the roughness variation is controlled to within 22% (based on BET surface area).[8] These core-toner particles are then treated with external additives to produce a final toner particle with the desired electrostatic charging, transfer efficiency, powder cohesion, and print image quality.

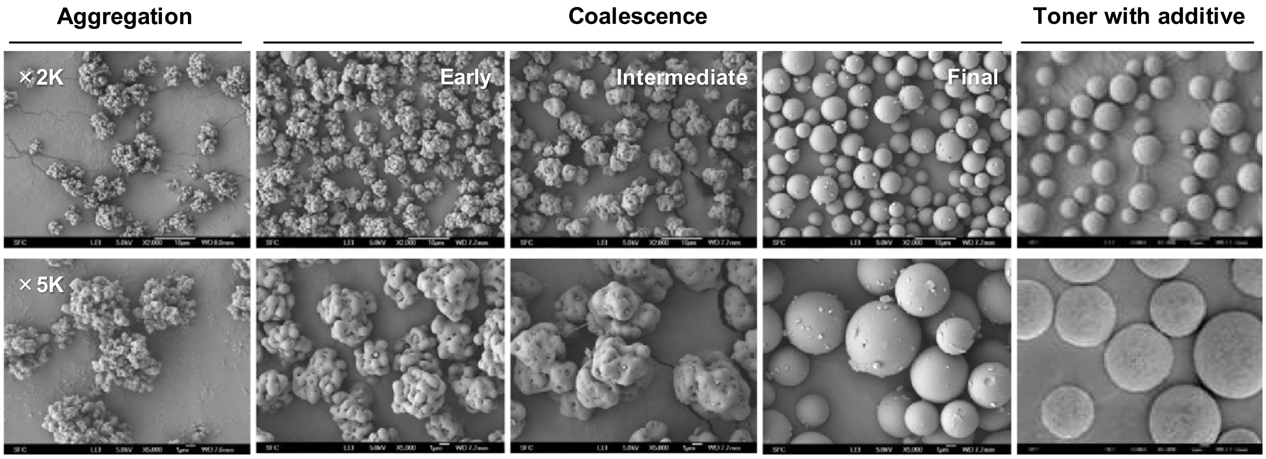

Figure 4. Toner particle morphology for each process stage. Each SEM image represents the particle morphology at the aggregation, early coalescence, intermediate coalescence, and final coalescence stages. An additional image of the final toner product (toner with additive) is presented.

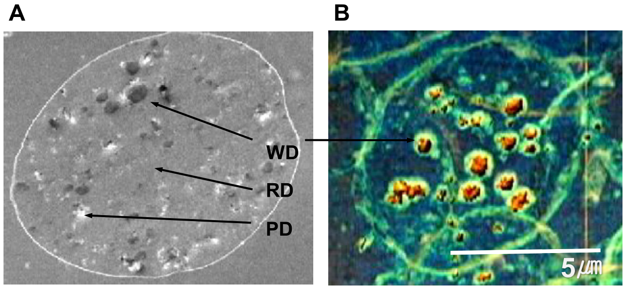

Figure 5. Intrastructure of toner particles. TEM (A) and 3D electron tomography (B) images of toner featuring the wax dispersion (WD), resin dispersion (RD), and pigment dispersion (PD).

Figures 5A and B illustrate the internal structure of core-toner particles that were examined via TEM and 3D electron tomography. The tomographs show a uniform distribution of resin, pigment, and wax within each toner particle (dispersion size ~ 2 μm, random locations). The literature reports that a poor wax or pigment dispersion is one source of poor toner durability. The dispersed size and uniformity of the wax in the SFC toner are much better than conventional mechanically prepared toners.[19]

Toner properties that are related to printing—that is, fusing offset, adhesion to paper, electrostatic charging, and environmental durability—are adjustable to match the level for various OEM printer models (data not shown). An additional quality that our toners provide is eco-friendliness due to their water-based manufacturing process and compatibility with energy efficient laser printer models that utilize a low temperature toner fusing process. Table III lists the main volatile organic components found in toners. The low total VOC emission levels of our toners meet the European Union's Blue Angel Criteria (certified analysis performed on SFC-CPT by the Landesgewerbeanstalt Bayern (LGA) Institute).[8,11]

Table III. LGA test results of volatile organic emission.

Parameter	Limiting value (mg/kg)	SFC-CPT values (mg/kg)
TVOC[a]	<300	248
Benzene	<0.35	<0.3
Styrene	<40	0.6
Volatile CMR[b] substances	<1.0	<0.3

[a] TVOC: Total volatile organic compounds.

[b] CMR: Carcinogenic, mutagenic, reproductive, and toxic substances.

Print Performance of SFC Toner

Table IV lists the print performance results for SFC toner based on a modified ISO and ASTM printing test protocol. SFC toner showed equivalent performance when compared to an OEM toner that was specifically designed for a designated printer model in terms of toner usage and image quality. The image quality values—that is, the image density and uniformity, fusing efficiency, ghost, and background—proved that the printing performance of SFC toner is equivalent to that of HP toner. These data were provided to our potential customers to illustrate the performance of SFC color toners relative to their OEM counterparts.

CONCLUSION

Digital printing technologies have matured to complement and personalize industrial printing technologies such as offset and gravure methods.[20] As the usage of office color laser printers and high speed multi-functional printers increases, the demands for high quality images and smaller environmental footprint are driving most toner manufacturers to develop eco-friendly polyester-based CPT.[4,21] The effect of the cationic valence on the aggregation process seems to be critical to the viscosity of the reactant which is required in achieving a narrow particle size distribution. In addition, the cationic valence and the acidity of the reactant also affect the aggregation of particles. Our ability to accurately control the aggregation behavior of polyester-based colloidal particles in an aqueous system and to produce a uniform circular toner with a narrow particle size distribution demonstrates that SFC is ready to support any OEM printer engine manufacturer in developing toners for their new printer

Table IV. Printing performances of SFC toner using HP CP4525.

Description	Reference	SFC Toner			
		Black	Cyan	Magenta	Yellow
Toner usage					
Toner consumption (mg/page)[a]	<14.0	14.6	14.4	13.1	11.8
Transfer efficiency (%)[a,b]	$>90\%$	85.8	90.0	89.1	91.6
Toner weight at EOL[c] (g)	—	49.4	36.5	22.4	33.1
Image quality					
Image density	~ 1.2	1.25	1.22	1.26	1.28
Density uniformity[d]	—	0.01	0.10	0.10	0.10
Fusing efficiency (%)[e]	$>95\%$	99.5	99.4	99.6	99.5
Ghost[f]	OK	OK	OK	OK	OK
Background[g]	Low	0.00	0.00	0.00	0.00

[a] Data are average values of 13,000 printouts (black) and 9,000 printouts (color).

[b] Transfer efficiency evaluates the amount ratio of toner used on printout.

[c] End of life.

[d] Density uniformity is the maximum difference between the measured densities of solid images in a single printout.

[e] Fusing efficiency is relative image intensity of peel off image.

[f] Ghost evaluates the residual image of previous images.

[g] Background is an unexpected contamination of printout background.

models. We have demonstrated that the overall performance of our SFC-CPT is equivalent to the best OEM toners. The additional environmental benefits that our toners provide include an eco-friendly production process, the low level of TVOC, and the ability to use the polyester-based toners in low fusing temperature (low energy usage) printers.

ACKNOWLEDGMENTS

This research was supported by the R&D Center of Samsung Fine Chemicals Co., Ltd. The kind assistance of Na-Hyoung Kim, Hiromitsu Kikuchi, Zbig Tokarski, Il-Sun Hwang, and Hyun Jin (R&D Center, Samsung Fine Chemicals Co., Ltd.) in additive mixing and performance evaluation of SFC-CPT is acknowledged. Mino Yang from the Analytical Engineering Group, Samsung Advanced Institute of Technology collaborated in the analysis of internal structure by TEM and 3D electron tomography.[10]

REFERENCES

[1] D. Tyagi, "Toners for high quality digital production printing," *Proc. IS&T's DPP2003: Int'l Conf. on Digital Production Printing and Industrial Applications* (IS&T, Springfield, VA, 2003), pp. 207–210.

[2] T. Aoki, "Chemical toner technology and the future," *Proc. IS&T's NIP19: Int'l Conf. Digital Printing Technol.* (IS&T, Springfield, VA, 2003), pp. 2–4.

[3] G. J. Galliford, *Chemically Prepared Toners—A Study of Markets and Technologies*, 6th ed. (Galliford Consulting & Marketing), pp. 15–20.

[4] D. Tyagi, "Polyester-based chemically prepared toner for high-speed digital production printing," *Proc. IS&T's NIP23: Int'l. Conf. on Digital Printing Technol. and Digital Fabrication 2007* (IS&T, Springfield, VA, 2007), pp. 270–227.

[5] G. J. Galliford, *Chemically Prepared Toners—A Study of Markets and Technologies*, 6th ed. (Galliford Consulting & Marketing), pp. 72–83.

[6] M. Nakamura, Y. Arima, A. SugaWara, T. Tanabe, and T. Yano, "Toner for developing electrostatic image, method for producing the same, developer for developing electrostatic image, and image forming method," US Patent 7,846,633 B2 (2010); M. Takahashi, H. Hamano, A. SugaWara, M. Nakamura, and Y. Oya, "Electrostatic latent image developing toner and method for producing the same, and electrostatic latent image developer, toner cartridge, process cartridge and image forming apparatus," US Patent 7,906,264 B2 (2011).

[7] Y. Liang, N. Hilal, P. Langston, and V. Starov, "Interaction forces between colloidal particles in liquid: Theory and experiment," Adv. Colloid Interface Sci. **134–135**, 151–166 (2007).

[8] B. Y. Kim, D. W. Kim, S. Y. Kim, J. H. Lee, and K.-Y. Yon, "Polyester-based chemical toner with low level of total volatile organic compounds," *Proc. IS&T's NIP26: Int'l. Conf. on Digital Printing Technol. and Digital Fabrication 2010* (IS&T, Springfield, VA, 2010), pp. 77–80; E. H. Ryu, S. Y. Kim, I. H. Kim, and K.-Y. Yon, "Eco-friendly prepared chemical toner with mixed polyester resin," *Proc. IS&T's NIP26: Int'l. Conf. on Digital Printing Technol. and Digital Fabrication 2010* (IS&T, Springfield, VA, 2010), pp. 73–76.

[9] S. Y. Kim, D. I. Hwang, I. S. Hwang, B. Y. Kim, D. W. Kim, and S. S. Kim, "Method of preparing toner", PCT /KR2011/000738 PX038638 (2011); E. H. Ryu, I. S. Hwang, I. H. Kim, and S. Y. Kim, "Method of preparing environment-friendly toner," PCT/KR2011/002299 PX038912 (2011).

[10] M. Yang, J.-H. Lee, H.-G. Kim, E. Kim, Y.-N. Kwon, J.-K. Kim, and C.-W. Yang, "Meso-scale transmission electron microscope tomography applied for wax distribution in toner particles," Microsc. Microanal. **19**, 58–61 (2013) Supplement S5.

[11] K. Berger and T. Nakamura, "Blue angel award criteria for electrophotographic toner," *Proc. IS&T's NIP21: Int'l. Conf. on Digital Printing Technol.* (IS&T, Springfield, VA, 2005), pp. 521–524.

[12] N. Kovalchuk, V. Starov, P. Langston, and N. Hilal, "Formation of stable clusters in colloidal suspensions," Adv. Colloid Interface Sci. **147–148**, 144–154 (2008).

[13] S. B. Hall, J. R. Duffield, and D. R. Williams, "A reassessment of the applicability of the DLVO theory as an explanation for the Schulze–Hardy rule for colloid aggregation," J. Colloid Interface Sci. **143**, 411–415 (1991).

[14] P. N. Jonson and A. Amirtharajah, "Ferric chloride and alum as single and dual coagulants," J. Am. Water Works Assoc. **75**, 232 (1983).

[15] A. Amirtharajah and K. M. Mills, "Rapid-mix design for mechanisms of alum coagulation," J. Am. Water Works Assoc. **74**, 210 (1992).

[16] J. A. Dean, *Lange's Handbook of Chemistry*, 14th ed. (McGraw-Hill, Inc., 1992), 8.83–88, 8.3–8.

[17] B. V. Deryaguin, N. V. Churaev, and V. M. Muller, *Surface Forces* (Consultants Bureau, Plenum Press, New York, 2005).

[18] P. W. Atkins, *Physical Chemistry*, Oxford, 5th ed. 974–976 (1994); B. Dobias, *Coagulation and Flocculation* (Marcel Dekker, New York, 1993).

[19] J. Shimizu, S. Omatsu, and Y. Hidaka, "The pulverized full-color toner with high performances," *Proc. IS&T's NIP19: Int'l. Conf. on Digital Printing Technol.* (IS&T, Springfield, VA, 2003), pp. 130–133; A. Eida, S. Omatsu, and J. Shimizu, "The advanced color toner for the fine image quality," *Proc. IS&T's NIP20: Int'l. Conf. on Digital Printing Technol.* (IS&T, Springfield, VA, 2004), pp. 102–106.

[20] M. Slot, "The future of research and development in the digital printing industry," *Proc. IS&T's NIP25: Int'l. Conf. on Digital Printing Technol. and Digital Fabrication 2009* (IS&T, Springfield, VA, 2009), p. 1.

[21] A. Eida, S. Omatsu, and J. Shimizu, "The advanced color toner for the fine image quality," *Proc. IS&T's NIP20: Int'l. Conf. on Digital Printing Technol.* (IS&T, Springfield, VA, 2004), pp. 102–106.